

Particle astrophysics from the cold: Results and perspectives of IceCube

C. de los Heros
(for the IceCube collaboration)* ¹

Department of Physics and Astronomy, Uppsala University, Uppsala, Sweden.

We discuss results of the AMANDA neutrino telescope, in operation at the South Pole since 2000, and present the status and scientific potential of its km³ extension, IceCube.

1.1 Introduction

In 1931 Victor Hess founded a research station 2300m up at the Hafelekar mountain, not very far from the premises of this meeting, for observing and studying cosmic rays. Hess received the Nobel Prize in Physics in 1936 for the discovery of “cosmic radiation”, and in his Nobel lecture he already identified the key to the development of the new opened field “In order to make further progress, particularly in the field of cosmic rays, it will be necessary to apply all our resources and apparatus simultaneously and side-by-side” [1]. Seventy years after his words, the field of astroparticle physics has come to maturity precisely from the close cooperation of optical and gamma ray telescopes, air shower arrays and neutrino telescopes.

Acceleration of particles to the extreme energies detected today (up to 10²⁰ eV) is assumed to be driven by shock fronts propagating in hot and dense regions of ionized matter. Such conditions are expected to be found in the neighborhood of accreting objects, like AGN or micro-quasars, or in extreme explosions like Gamma Ray Bursts (GRBs). There are compelling theoretical arguments to expect neutrino production from these

¹ Prepared for the proceedings of the first AFI symposium, Innsbruck, 19-20/10/2007 . To be published by Innsbruck University Press. Eds S. D. Bass, F. Schallhart and B. Tasser

sites as well. Accelerated protons must interact with the ambient matter or radiation, producing secondary charged pions and kaons which decay to neutrinos. Neutral pions will also be produced and they will decay into $\gamma\gamma$, giving a normalization of the neutrino flux with the gamma ray flux. A neat example of the need for “using apparatus simultaneously” mentioned by Hess.

In this proceedings we will present results from the AMANDA neutrino telescope on the searches for cosmic neutrinos and discuss the status and first physics results from its km^3 successor, IceCube. Neutrino telescopes are not only astrophysical instruments, but can be used to address topics in cosmology and particle physics. We will also report on the AMANDA results on searches for WIMPs, monopoles and non-standard oscillation scenarios.

1.2 The AMANDA and IceCube detectors

As of January 2008, the IceCube Neutrino Observatory [2] is close to half size of its final design and it is already the largest neutrino telescope in the world. The observatory consists of a 1 km^3 ice array, IceCube, and a surface air-shower array, IceTop. The ice array will consist of up to 80 strings holding 60 digital optical modules (DOMs) each, deployed at depths between 1450 m - 2450 m near the geographic South Pole. The DOMs are vertically separated by 17 m, while the strings are arranged in a triangular grid with an inter-string separation of 125 m. Each IceCube DOM contains a 25-cm Hamamatsu photomultiplier tube with electronics for in-situ digitization and timing of the photomultiplier waveforms, as well as a LED flasher board for calibration purposes. The observed dark noise rate of the DOMs is about 700 Hz.

IceCube is designed to detect the Cherenkov radiation of secondaries produced in neutrino interactions. For the ν_μ channel, the Earth is used as a filter and only up-going muon tracks are considered, due to the overwhelming down-going atmospheric muon background. The detector monitors therefore the northern sky. For the ν_e and ν_τ channels, the signature is the particle cascade produced in the neutrino interactions close or inside the detector, and the whole sky can then be monitored.

The IceTop surface array uses the same DOM architecture as IceCube. The array will consist of 80 stations, one near the surface location of each IceCube string. A station consists of two ice tanks, with two DOMs in each one operated at different gains to increase the tank dynamic range. IceTop will detect the charged particle component of air showers above 10^{14} eV.

Historically, the first neutrino detector at the South Pole was AMANDA. Completed in 2000, the detector consists of 677 optical modules (20-cm photomultiplier tubes housed in glass spheres), deployed in 19 strings at depths between 1450 m and 2000 m. The strings are arranged in three approximately concentric circles of 40 m, 100 m and 200 m in diameter. The AMANDA optical modules are simpler than the IceCube DOMs, not containing any embedded digitizing hardware. Signal processing and triggering is done at the surface. AMANDA was fully incorporated into the IceCube detector as a subsystem in 2007 and it is now part of the IceCube trigger system. With its denser string spacing (typically 30 m) AMANDA can be used as a low energy array. IceCube strings surrounding AMANDA can be used as a veto to define contained events, lowering the energy threshold to a few tens of GeV.

1.3 Results from AMANDA

1.3.1 The Galactic plane

Cosmic rays interacting with the interstellar medium in the galaxy are a source of guaranteed neutrinos, produced through secondary pion and kaon decays. From the geographical location of AMANDA, only the outer region of the galactic plane, between longitude $33^\circ < \delta < 213^\circ$, lies below the horizon and can therefore be monitored. We have searched the data collected between 2000 and 2003, 3329 neutrino events, for a possible enhancement of the neutrino flux from the galactic disk. Assuming a Gaussian shape of the distribution of matter in the galactic disk, with a width of 2.1° , and a $E_\nu^{-2.7}$ spectrum, we obtain a 90% CL limit on the neutrino flux of 4.8×10^{-4} $\text{GeV}^{-1} \text{cm}^{-2} \text{sr}^{-1} \text{s}^{-1}$ in the range $0.2 \text{ TeV} < E_\nu < 40 \text{ TeV}$ [3].

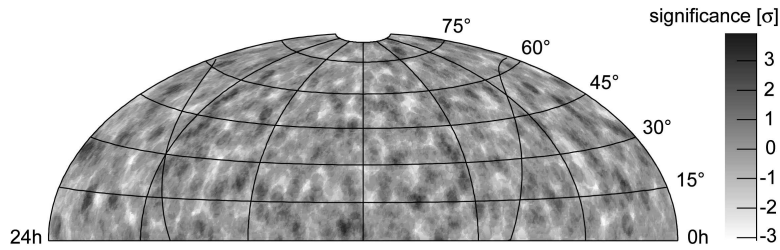


Figure 1.1. Significance sky map using 5 years of AMANDA data. The figure shows the deviation from a uniform background.

1.3.2 Searches for a cosmic neutrino flux

a) Steady Point sources: The search for point sources of neutrinos is performed by looking for statistical excesses of events in narrow angular regions in the sky, determined by the angular resolution of the detector (about 2° for this analysis). The search can be done in a generic way, looking for “hot spots” with respect to the average background, or by looking at the position of predefined candidate objects. In the latter case, the background is estimated from the data off-source, in the same declination band as the candidate object. These searches are done exclusively for muon neutrinos due to the better pointing resolution, and therefore are restricted to the northern sky. However the search is also sensitive to tau neutrinos through the muon produced in the tau decay, so the upper limits in table 1.1 refer to the combined flux $\Phi_{\nu_\mu} + \Phi_{\nu_\tau}$. See [4] for details.

The results mentioned here were obtained with the combined data sets of the years 2000-2004. It amounts to a total of 1001 days of live-time, and the sample contains 4282 upward going neutrino events. Figure 1.1 shows the significance map of the northern sky in galactic coordinates. The map is compatible with a random distribution of sources, the hottest spot having a 92% probability of being a random fluctuation.

The same data set has been used to search for a neutrino flux from the direction of known objects. For this search we have used 32 sources known to be gamma and/or X-ray emitters, like Blazars, micro-quasars or supernova remnants. Table 1.1 shows the neutrino flux limits obtained for a few selected sources assuming an E^{-2} neutrino energy spectrum [4].

The sensitivity for point sources can be increased by using a source-stacking analysis, where the data from the directions of sources known to

Candidate	$\delta(^{\circ})$	$\alpha(\text{h})$	n_{obs}	n_b	Φ_{ν}^{lim}	Candidate	$\delta(^{\circ})$	$\alpha(\text{h})$	n_{obs}	n_b	Φ_{ν}^{lim}
<i>TeV Blazars</i>						<i>GeV Blazars</i>					
Markarian 421	38.2	11.1	6	7.4	7.4	QSO 0219+428	42.9	2.4	5	5.5	9.6
Markarian 501	39.8	16.9	8	6.4	14.7	QSO 0954+556	55.0	9.9	2	6.7	2.7
<i>Micro-quasars</i>						<i>SNR & Pulsars</i>					
SS433	5.0	19.2	4	6.1	4.8	SGR 1900+14	9.3	19.1	5	5.7	7.8
Cygnus X3	41.0	20.5	7	6.5	11.8	Crab Nebula	22.0	5.6	10	6.7	17.8
GRS 1915+105	10.9	19.3	7	6.1	11.2	Geminga	17.9	6.6	3	6.2	3.5
Cygnus X1	35.2	20.0	8	7.0	13.2	Cassiopeia A	58.8	23.4	5	6.0	8.9

Table 1.1. $\nu_{\mu} + \nu_{\tau}$ flux limits from selected objects. δ is the declination in degrees, α the right ascension in hours, n_{obs} is the number of observed events and n_b the expected background. Φ_{ν}^{lim} is the 90% CL upper limit on the flux of muon plus tau neutrinos in units of $10^{-8} \text{ GeV}^{-1} \text{ cm}^{-2} \text{ s}^{-1}$ for a spectral index of 2 and integrated above 10 GeV.

have similar morphological characteristics are added. The background for each object is estimated off-source from the same zenith band as the location of the object, and added for all candidates. A preliminary analysis performed with data collected in 2000-2003 for several types of sources shows no excess over the expected Poisson statistics [5].

b) Diffuse neutrino flux: Even if the neutrino flux from individual sources would be too weak to be detected with a detector of the size of AMANDA, a diffuse flux of neutrinos from the injected spectrum of all sources in the Universe could be detectable. The search for such flux is a challenge since it is, by definition, not correlated in time or position with any particular object. The search is based on the expected harder neutrino spectrum, $d\Phi/dE_{\nu} \propto E_{\nu}^{-2}$, from the shock-acceleration of protons in the source, as compared to the $E^{-3.7}$ dependence of the atmospheric neutrino flux. In analysis terms, this translates in exploiting the different shapes of the distribution of the number of optical modules hit, a variable related to the energy of the event. This search can be done both for ν_{μ} and cascades from ν_e and ν_{τ} , and can cover a wide range of energies, from a few tens of TeV to EeV. Above PeV energies, the Earth becomes opaque to neutrinos and the search has to be concentrated on events from near or above the horizon.

The most recent limit obtained by AMANDA for muon neutrinos is based on the analysis of four years of data (2000-2003), with a total lifetime of 807 days [9]. The absence of a signal is translated to a limit on the

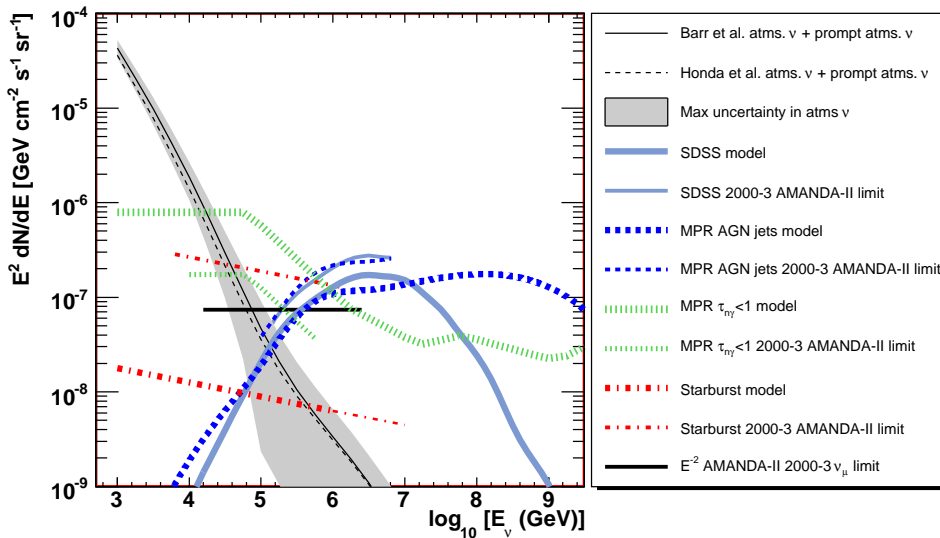


Figure 1.2. AMANDA upper limits from the diffuse analysis. The Barr *et al.* and Honda *et al.* atmospheric neutrino models are shown as thin lines with uncertainties represented by the band. Other models that were tested included the SDSS AGN core model [6], the MPR upper bounds for AGN jets and optically thin sources [7], and a starburst galaxy model [8].

diffuse muon neutrino flux of $E_\nu^2 d\Phi/dE_\nu < 7.4 \times 10^{-8} \text{ GeV cm}^{-2} \text{ s}^{-1} \text{ sr}^{-1}$ in the energy range 16 TeV–2.5 PeV. Other spectral shapes predicted by different theoretical models [6, 7, 8] were also tested and limits set, as shown in figure 1.2. See [9] for details.

A search for a diffuse flux in the cascade channel (sensitive to all flavours and with 4π acceptance) is under way using 1000 days of live-time collected during 2000 to 2004. Using 20% of the data set a sensitivity on a ν_e flux of $2.7 \times 10^{-7} (E_\nu/\text{GeV})^{-2} \text{ GeV cm}^{-2} \text{ s}^{-1} \text{ sr}^{-1}$ has been obtained [10].

In the ultra-high energy regime, $E_\nu \gtrsim \text{PeV}$, a search has been carried out on the 571 days of lifetime collected between 2000 and 2002 for a signal near the horizon. No statistically significant excess above the expected background has been seen, and 90% CL upper limit on the diffuse all-flavor neutrino flux of $E_\nu^2 d\Phi/dE_\nu < 2.7 \times 10^{-7} \text{ GeV cm}^{-2} \text{ s}^{-1} \text{ sr}^{-1}$ has been obtained, valid over the energy range of $2 \times 10^5 \text{ GeV}$ to 10^9 GeV [11].

Gamma-ray bursts: A rather special type of candidate neutrino point source is Gamma Ray Bursts (GRB), since for these objects one can have the time stamp and coordinates of the event from other detectors. This

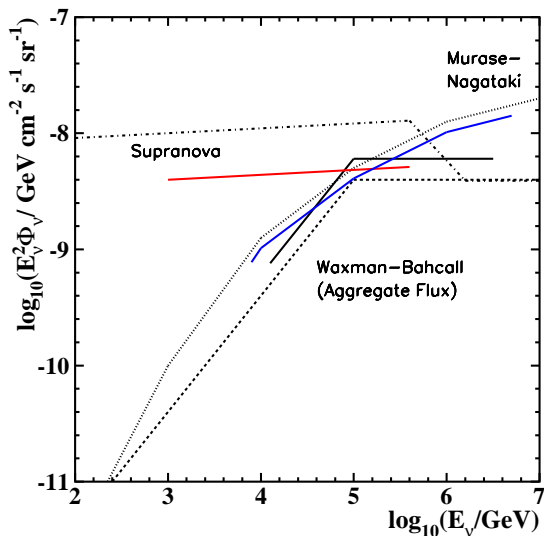


Figure 1.3. AMANDA GRB flux upper limits (solid lines) for ν_μ energy spectra predicted by the Waxman-Bahcall spectrum (thick dashed line) [14], the Razzaque et al. spectrum (dot-dashed line) [15] and the Murase-Nagataki spectrum (thin dotted line) [16].)

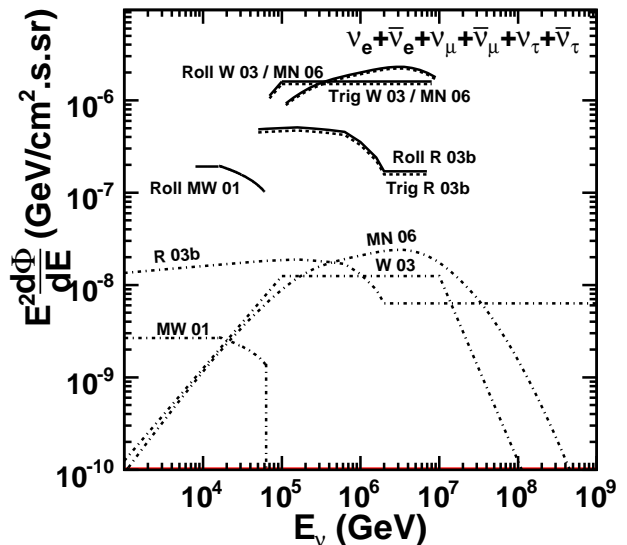


Figure 1.4. Predicted GRB all-flavor neutrino fluxes compared to AMANDA cascade analysis limits (*Rolling* limits (Roll) in solid line and *Triggered* limits (Trig) in dashed line). Models shown are: [14] (W 03), [17] (R 03b), [16] Model A (MN 06) and [18] (MW 01).

allows one to perform a practically background-free analysis using both off-source and off-time background estimation. An additional advantage of having the time stamp of the event is that the required pointing resolution can be relaxed and then the cascade channel can be used, giving access to full-sky searches. Additionally, a “rolling search” can also be performed where no trigger information from any external detector is used and AMANDA data are searched for events clustered in short time periods. We have performed three GRB search analyses, one for muon neutrinos [12] and two using the cascade channel [13]. The triggered analyses rely on spatial and temporal correlations with photon observations of BATSE and several satellites of the Third Interplanetary Network (IPN).

The muon neutrino analysis has been performed using 419 GRB bursts between 1997 and 2003. No neutrinos were observed in coincidence with the bursts, resulting in the most stringent upper limit on the muon neutrino

flux from GRBs to date. Assuming a Waxman-Bahcall spectrum, a 90% CL upper limit of $E_\nu^2 d\Phi/dE_\nu \leq 6.0 \times 10^{-9} \text{ GeVcm}^{-2}\text{s}^{-1}\text{sr}^{-1}$, has been obtained, with 90% of the events expected within the energy range between 10 TeV and 3 PeV. We have also tested the flux predictions from several prominent GRB models based on averaged burst properties. The 90% C.L. flux upper limits relative to these models are shown in figure 1.3.

Concerning the cascade channel, we have performed two searches for neutrino-induced cascades. The triggered analysis searched for neutrinos in coincidence with 73 gamma-ray bursts reported by BATSE in 2000. The rolling analysis searched for a statistical excess of cascade-like events in time rolling windows of 1 s and 100 s in the period 2001 to 2003. The resulting limits are $E_\nu^2 d\Phi/dE_\nu \leq 1.5 \times 10^{-6} \text{ GeVcm}^{-2}\text{s}^{-1}\text{sr}^{-1}$ for the triggered analysis and $E_\nu^2 d\Phi/dE_\nu \leq 1.6 \times 10^{-6} \text{ GeVcm}^{-2}\text{s}^{-1}\text{sr}^{-1}$ for the rolling analysis. Lacking spatial and temporal constraints, the rolling analysis has a reduced per-burst sensitivity relative to triggered analyses. On the other hand, a rolling analysis has the potential to detect sources missed by other methods. The test of specific models using the cascade channel is shown in figure 1.4.

1.3.3 Search for dark matter candidates

Searches for dark matter with neutrino telescopes are based on searches for an excess neutrino flux from relic particles gravitationally accumulated in the Earth or the Sun. A massive (GeV-TeV range), weakly interacting and stable particle, the neutralino, appears in Minimally Supersymmetric extensions of the Standard Model that assume R-parity conservation, and it is a good candidate for non-baryonic dark matter. These relic particles, if accumulated in the center of the Sun or Earth, can annihilate pairwise, and neutrinos can result from the decays of the annihilation products [19]. We have performed searches for neutralino dark matter accumulated in the Earth (2001–2003 data set) [20], and the Sun (2001 data set) [21]. The results are shown in figure 1.5. The figures show the muon flux limit from neutralino annihilations, along with the results from other indirect searches and predictions from theoretical models. Disfavoured models by recent direct searches [22] are shown as (green/grey) dots.

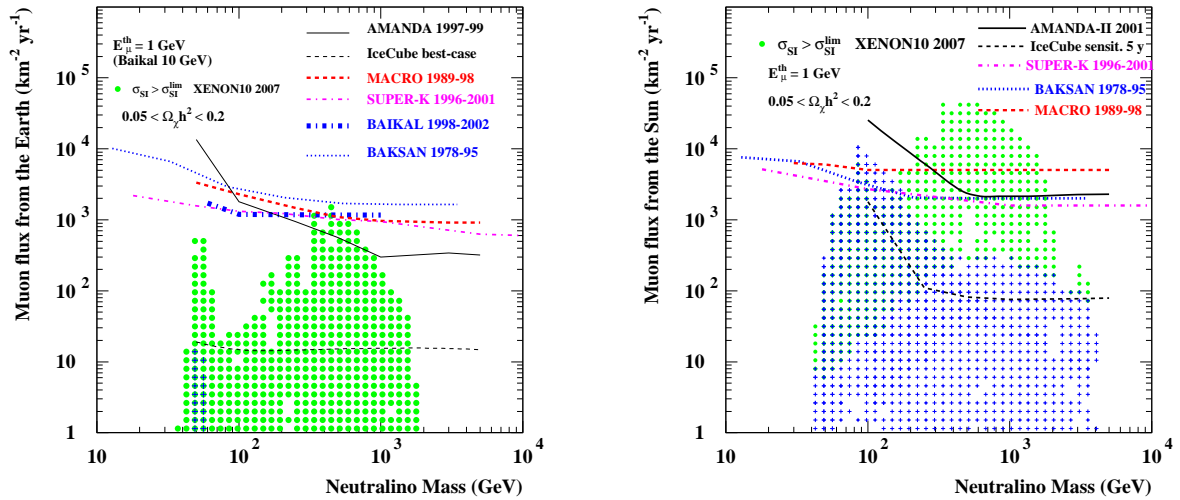


Figure 1.5. 90% CL upper limit on the muon flux from neutralino annihilations in the center of the Earth (left) and from the Sun (right). Markers show predictions for cosmologically relevant MSSM models, the dots representing models excluded by XENON10 [22].

1.3.4 Magnetic monopoles and exotics

Stable magnetic monopoles with masses in the range between 10^8 to 10^{17} GeV are predicted in Grand Unified Theories [23]. They can be accelerated by large scale magnetic fields, and those with masses below $\sim 10^{14}$ GeV can acquire relativistic speeds. Their Cherenkov emission in ice is enhanced by a factor 8300 $((n/2\alpha)^2$, where n is the refractive index and α is the electromagnetic coupling constant), compared to a particle with unit electric charge and the same speed. This constitutes the main experimental signature of monopoles in neutrino telescopes: extremely bright events. Monopoles with masses above 10^{11} GeV can cross the entire Earth and enter the detector from below, allowing for a search of up-going particles, practically background free.

We have analyzed data taken with AMANDA during the year 2000 in search for monopole candidates [24]. For monopole speeds greater than $\beta = 0.8$ and masses greater than $\sim 10^{11}$ GeV, the flux limit is presently the most stringent experimental limit. Figure 1.6 shows the flux limits set by AMANDA compared to those set by MACRO [25] and by BAIKAL [26].

Supermassive monopoles will remain sub-relativistic and do not pro-

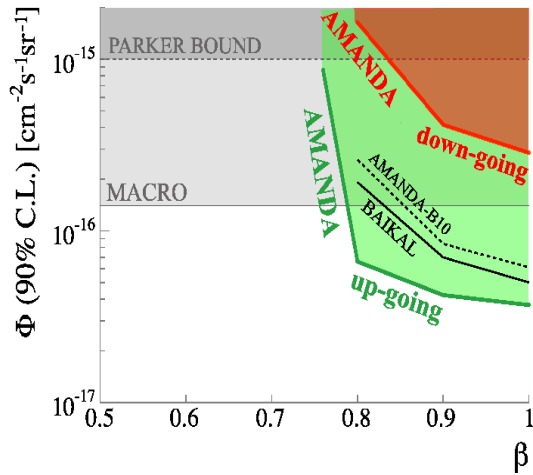


Figure 1.6. Preliminary limits on the flux of relativistic magnetic monopoles set by AMANDA. Earlier AMANDA (marked AMANDA-B10), MACRO and BAIKAL results are also shown.

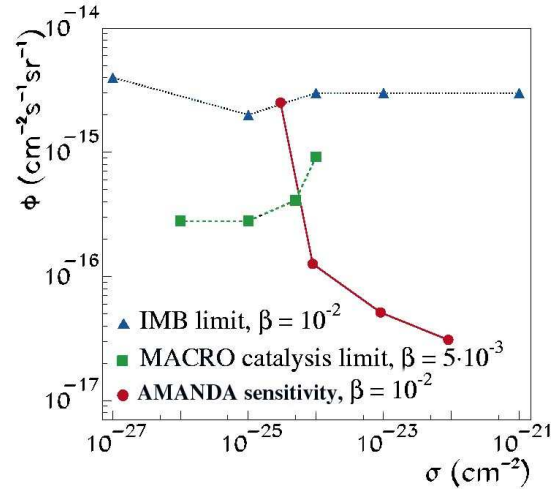


Figure 1.7. Preliminary AMANDA sensitivity to sub-relativistic particles as a function of varying catalysis cross section. Limits set by IMB and MACRO are also shown.

duce Cherenkov radiation when passing through ice. However, they can be detected through nucleon decay catalysis: the charged decay products (e 's, π 's, μ 's and K 's) will emit Cherenkov radiation along the monopole trajectory. A similar process applies for neutral Q-balls, another type of relic massive particles [27]. In a neutrino telescope, the signature of catalyzing particles would be a series of closely spaced electromagnetic showers produced along the particle trajectory. The detection of slow particles builds on the fact that relativistic muons emit light during $\sim 3 \mu\text{s}$ (the time it takes to cross the AMANDA volume), whereas slow particles would emit during a large fraction of the $33 \mu\text{s}$ time window of the AMANDA data acquisition system. The sensitivity of a preliminary search for sub-relativistic particles in 113 days of lifetime in 2001 [30] is shown in figure 1.7, along with existing limits from other experiments [28, 29].

1.3.5 Search for non-standard neutrino oscillations

Some phenomenological models of physics beyond the Standard Model predict flavour mixing in the neutrino sector in addition to the standard mass-induced oscillations [31]. In particular, violation of Lorentz Invariance can

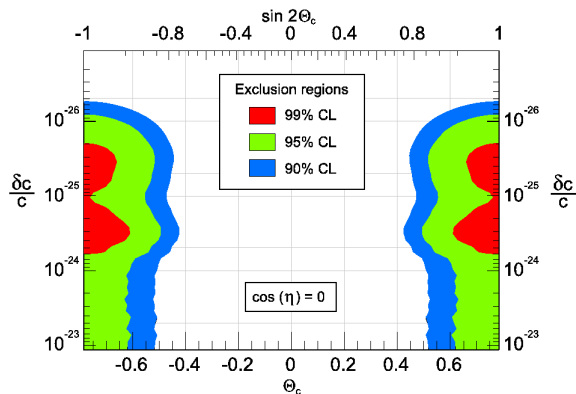


Figure 1.8. Preliminary exclusion regions for $\delta c/c$ as a function of the mixing angle Θ

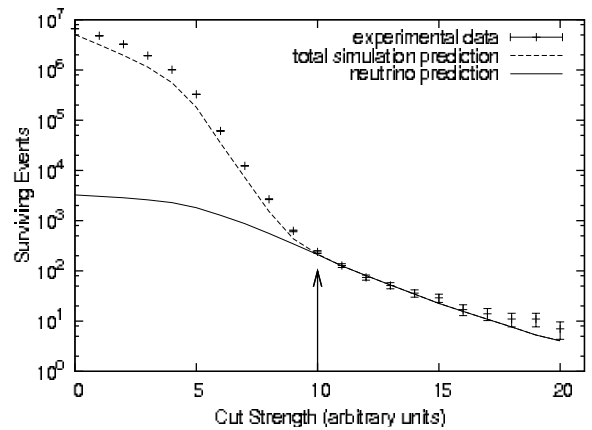


Figure 1.9. Number of events remaining for data, atmospheric muons and atmospheric neutrinos as a function of increasing event quality criteria.

lead to different maximum attainable velocities (MAV) for the different flavours, and therefore to MAV-induced oscillations, since MAV eigenstates will not be flavour eigenstates. The effect can be parametrized in terms of $\delta c/c$, the difference in maximal attainable velocity. In contrast to mass-induced oscillations, MAV oscillations show a linear energy dependence of the oscillation frequency. The expected signature in AMANDA/IceCube is a distortion of the angular and energy spectra of atmospheric neutrinos at energies above 10^5 GeV.

We have used data collected between 2000 and 2003 to search for anomalous oscillation effects in 3401 atmospheric neutrinos collected in that period [32]. The exclusion regions of $\delta c/c$ as a function of the mixing angle Θ_c at different confident levels are shown in figure 1.8, for a particular value of the unconstrained phase η . However the results can be shown to be quite insensitive to the value of η .

1.4 First results and perspectives from IceCube

IceCube is growing rapidly. The detector took data with 9 strings during 2006 and, after the deployment season during the austral summer 2006/07, it consists of 22 strings and a total of 1320 DOMs. In addition 26 IceTop tanks are operational. With 98% of the DOMs deployed so far commis-

sioned and working, the detector parameters meet or exceed the design specifications. Construction is on schedule and foreseen to be completed by 2011.

The data from 137 days of lifetime accumulated during 2006 has been analyzed and the first atmospheric neutrino candidates identified, a total of 234 for an expected yield of $211 \pm 76(\text{syst.}) \pm 14(\text{stat.})$ from a pure atmospheric neutrino flux [33]. Figure 1.9 shows the number of data events, atmospheric muon background and atmospheric neutrinos remaining as a function of increasing event quality selection. Figure 1.10 shows the zenith angle distribution of the 234 events. Some residual atmospheric muons remain near the horizon, but the sample is consistent with the atmospheric neutrino angular distribution (shown as a grey band including theoretical uncertainties in the expected flux and systematic uncertainties in the detector response) for declinations above $\sim 120^\circ$. The data was also searched for “hot spots” due to point sources [34], and a preliminary significance sky map obtained, as shown in 1.11. The resulting preliminary sky-averaged point-source sensitivity for an E^{-2} spectrum is $E_\nu^2 d\Phi/dE_\nu = 12 \times 10^{-8} \text{ GeVcm}^{-2} \text{ s}^{-1}$, already comparable with the results of 5 years of AMANDA data (see table 1.1).

The sensitivity of IceCube to the different physics topics that can be addressed will increase rapidly as exposure and size increase during construction. The expected sensitivity to a diffuse flux of the complete detector after one year of data taking is $E_\nu^2 d\Phi/dE_\nu \sim 8.0 \times 10^{-9} \text{ GeVcm}^{-2}\text{s}^{-1}\text{sr}^{-1}$, an order of magnitude below the current AMANDA limit (obtained with three years of exposure). A similar improvement is expected in the sensitivity to point sources, not only due to the bigger effective volume but also due to the expected sub-degree angular resolution at TeV energies.

The possibility to identify flavour is one of the significant improvements of the capabilities of IceCube with respect to AMANDA. IceCube will be able to identify the typical “double-bang” signature of ν_τ events, the hadronic shower at the interaction vertex and the τ decay shower. Above PeV energies a tau can travel (O)100 m, and the separation of the two showers can be resolved. AMANDA is too small for this.

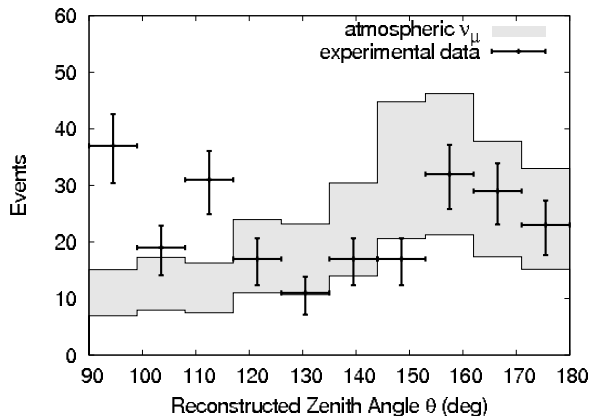


Figure 1.10. Zenith angular distribution of the 234 neutrino candidates in the IceCube 2006 data set.

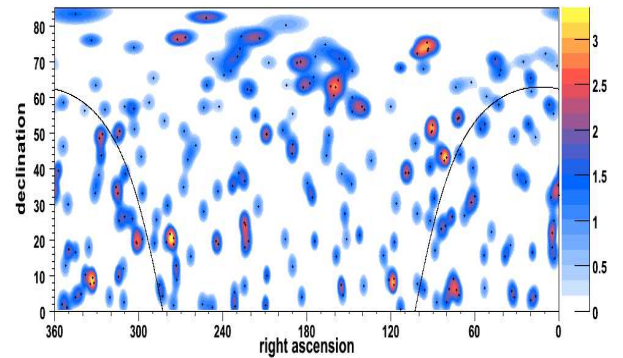


Figure 1.11. Significance sky map using 137 days lifetime of IceCube data in 2006. The figure shows the deviation from a uniform background.

1.5 Future extensions

There are ongoing plans to extend the capabilities of IceCube both at lower energies and at higher energies. On the low energy side we will build a compact core of 6 strings in the middle of the IceCube array, with typical inter-string separation of ~ 50 m. This allows us to use the surrounding strings as a veto region in order to define contained events and reduce the atmospheric muon background. Such a compact core will make it possible to increase the sensitivity to events below 100 GeV, an important energy range for the dark matter searches. The ability to reduce the background in such way will allow us to “look” to the Sun continuously, even when above the horizon. This also opens the possibility of looking at the Galactic center.

Above neutrino energies of $\sim 10^{18}$ eV the radio and acoustic signal of the particle cascade produced at the neutrino-nucleon interaction point dominates over the optical Cherenkov emission. Ice is extremely transparent to both radio and acoustic signals in the frequency ranges of interest (MHz-GHz for radio, kHz for acoustic), with attenuation lengths of the order of km in both cases. Two exploratory projects, AURA (Askaryan Under ice Radio Array) [35] and SPATS (South Pole Acoustic Test Setup) [36] are being carried out to explore the characteristics of polar ice and to develop and assess different hardware options for a future hybrid array of 90 strings with 1 km spacing surrounding the current IceCube site.

References

* see www.icecube.wisc.edu/collaboration/authorlists/2007/5.html for full author list and acknowledgments.

- [1] V. Hess, Nobel Lecture, in *Nobel Lectures, Physics 1922-1944*. Elsevier Publishing, Amsterdam (1965).
- [2] A. Achterberg *et al.*, *Astropart. Phys.* **26**, 155, (2006).
- [3] J. L. Kelley, Proc. of ICRC05, Pune, India, **00**, 101, (2005).
- [4] A. Achterberg *et al.*, *Phys. Rev.* **D75**, 102001 (2007).
- [5] A. Gross *et al.*, in proceedings of ICRC05, Pune, India, (2005).
- [6] F. W. Stecker *et al.*, *Phys. Rev. Lett.* **66**, 2697 (1991); **69**, 2738(E) (1992); **72**, 107301, (2005).
- [7] K. Mannheim, R. J. Protheroe and J. P. Rachen, *Phys. Rev. D* **63**, 023003, (2000).
- [8] A. Loeb and E. Waxman, *J. Cosmol. Astropart. Phys.* JCAP05, 003 (2006).
- [9] A. Achterberg *et al.*, *Phys. Rev.* **D76**, 042008 (2007).
- [10] O. Tarasova, M. Kowalski and M. Walter, Proc. of ICRC07, Mérida, Mexico, (2007). arXiv:0711.0353, page 83.
- [11] M. Ackermann *et al.*, to appear in *Astrophys. Journal*. arXiv:0711.3022.
- [12] A. Achterberg *et al.*, to appear in *Astrophys. Journal*. arXiv:0705.1186.
- [13] A. Achterberg *et al.*, *Astrophys. Journal*. **664**, 397, (2007).
- [14] E. Waxman, *Nucl. Phys. B Proc. Supp.* **118**, 353, (2003).
- [15] S. Razzaque *et al.*, *Phys. Rev.* **D68**, 3001, (2003).
- [16] K. Murase and S. Nagataki, *Phys. Rev.* **D73**, 063002, (2006).
- [17] S. Razzaque, P. Meszáros and E. Waxman, *Phys. Rev. Lett.* **90**, 241103, (2003).
- [18] P. Meszáros and E. Waxman, *Phys. Rev. Lett.* **87**, 171102, (2001).
- [19] G. Jungman, M. Kamionkowski and K. Griest, *Phys. Rep.* **267**, 195, (1996).
- [20] A. Achterberg *et al.*, *Astropart. Phys.* **26**, 129, (2006).
- [21] M. Ackermann *et al.*, *Astropart. Phys.* **24**, 459, (2006).
- [22] J. Angle *et al.*, arXiv:0706.003, (2007).
- [23] G. 't Hooft, *Nucl. Phys.* **B79**, 276, (1974).
- [24] H. Wissing, Proc. of ICRC07, Mérida, Mexico, (2007). arXiv:0711.0353, page 139.
- [25] M. Ambrosio *et al.*, *Eur. Phys. J.* **C25**, 511, (2002).
- [26] The BAIKAL Collaboration, Proc. of ICRC05, Pune, India (2005).
- [27] A. Kusenko *et al.*, *Phys. Rev. Lett.* **80**, 3185, (1998).
- [28] M. Ambrosio *et al.*, *Eur. Phys. J.* **C26**, 163, (2002).
- [29] R. Becker-Szendy *et al.*, *Phys. Rev.* **D49**, 2169, (1994).
- [30] A. Pohl and D. Hardtke, Proc. of ICRC07, Mérida, Mexico, (2007). arXiv:0711.0353, page 143.
- [31] S. Coleman and S. L. Glashow, *Phys. Lett* **B405**, 249, (1997).
- [32] J. Ahrens and J. L. Kelley, Proc. of ICRC07, Mérida, Mexico, (2007). arXiv:0711.0353, page 55.
- [33] A. Achterberg *et al.*, *Phys. Rev.* **D76**, 027101, (2007).
- [34] C. Finnley, J. Dumm and T. Montaruli, Proc. ICRC07, Mérida, Mexico, (2007). arXiv:0711.0353, page 107.
- [35] H. Landsman, L. Ruckman and G. S. Varner, Proc. of ICRC07, Mérida, Mexico, (2007). arXiv:0711.0353, page 163.
- [36] S. Böser *et al.*, Proc. of ICRC07, Mérida, Mexico, (2007)